JOURNAL OF PROPULSION AND POWER
Vol. 21, No. 4, July–August 2005

Thrust Chamber Dynamics and Propulsive Performance of Multitube Pulse Detonation Engines

Fuhua Ma,* Jeong-Yeol Choi,† and Vigor Yang‡
Pennsylvania State University, University Park, Pennsylvania 16802

Our earlier work on single-tube airbreathing pulse detonation engines (PDEs) is extended to explore the chamber dynamics and propulsive performance of multitube PDEs with repetitive operations. Detailed flow evolution in the entire chamber for two different configurations is examined over a broad range of operating parameters, and loss mechanisms are quantified. Emphasis is placed on the interactions between detonation tubes and their collective influence on the nozzle flowfield. The benefits of precompression of refilled fresh reactants by shock waves originating from other tubes are demonstrated. Compared with single-tube designs, multitube PDEs improve propulsive performance, reduce axial-flow oscillation, and offer a wider operation range in terms of valve timing. They can, however, cause thrust variation in the transverse direction. The convergent part of the nozzle helps preserve the chamber pressure and consequently improve the engine performance. The free volume between the detonation tubes and the common nozzle might render in performance degradation because of the existence of complicated shock structures and recirculating flows.

Nomenclature

F_{sp}	=	specific thrust
I_{sp}	=	specific impulse
p	=	pressure
T	=	temperature
t	=	time
u	=	axial velocity
v	=	vertical velocity
x	=	axial coordinate
γ	=	ratio of specific heats
ρ	=	density
τ_{close}	=	valve-closed period during which valve is closed, for each detonation tube
τ_{cycle}	=	cycle period for each detonation tube
τ_{purge}	=	purging period for each detonation tube
τ_{refill}	=	refilling period for each detonation tube

I. Introduction

EXTENSIVE efforts have been applied to study the flow dynamics and propulsive performance of single-tube airbreathing pulse detonation engines (PDEs).[1,2] Results indicate that for a typical supersonic mission of a flight altitude of 9.3 km and Mach number of 2.1 the best possible specific impulse for the baseline configuration with a stoichiometric hydrogen/air mixture is about 3672 s, based on a single-parameter model with a constant ratio of specific heats.[2] Further improvements of the system design are required to render the PDE more competitive with other conventional steady engines. The purpose of the present work is to explore a configuration with multiple detonation tubes, which in principle features the following advantages:

1) Delivery of air from the inlet to multiple detonation tubes reduces the inlet loss associated with airflow stagnation during the period when none of the tubes are being filled. In single-tube PDEs, this period takes up a large part of the cycle time and can cause inlet unstart.

2) Exhaust from multiple detonation tubes discharging into a common nozzle provides a more stable nozzle flow by increasing the nozzle exit pressure, which is quite low in a single-tube PDE during the later part of the blowdown process and the purging and refilling stages.

3) The detonation wave from one tube can precompress the reactants in other tubes.

4) The purging and refilling processes are less coupled with the blowdown process, thus leading to a wider range of operation timing.

5) The overall engine operation frequency can be increased by a factor equal to the number of detonation tubes used. In addition, the degree of flow unsteadiness is reduced.

6) Potential utilization of fluidic thrust vectoring can be made.

The concept of multitube design dates back to 1950. Goddard[3] considered a valved deflagration-based pulse jet engine with multiple combustors. Bussing[4] proposed a rotary valve multitube PDE concept in 1995 by combining certain aspects of the Goddard design and the detonation process. The system consists of several detonation tubes coupled to an air inlet and fuel supply via a rotary valve. The valve isolates the steady operation of the air inlet and fuel system from the unsteady operation of the detonation tubes and allows the filling of fresh reactants in some of the tubes while detonation occurs in other tubes. A simple performance analysis, including the contributions from the inlet, mixer, combustor, and nozzle, was conducted by Bratkovich and Bussing[5] to examine the performance characteristics over a wide range of flight conditions. Hinkey et al.[6] experimentally demonstrated the operation of a dual-tube PDE, with a firing rate per tube up to about 12 Hz. Recently, a four-tube PDE was constructed by Schauer et al., serving as a testbed for studying detonation initiation, high-frequency operation, and wall heat transfer.[7] The system was modified from a 16-valve, four-cylinder automobile engine. A rotary position sensor was adapted to the intake camshaft to provide both an index of the valve timing sequence and the relative position of the valves. Each detonation tube could operate at frequencies up to 100 Hz.

Numerical investigations on multitube PDEs have also been conducted recently. Mohanraj et al.[8] presented an approximate model for a PDE with five detonation tubes. A time-accurate solution was obtained for the one-dimensional flowfield in one tube, with the situations in other tubes modeled using a time-delayed version of this solution. Their results showed that the filling process in a multitube PDE could be markedly different from that in a single-tube PDE. In particular, increasing the fill time does not affect the quantity of

Received 9 February 2004; revision received 21 December 2004; accepted for publication 20 December 2004.

*Postdoctoral Research Associate, Department of Mechanical Engineering; mafuhua@psu.edu.

†Visiting Assistant Professor, Department of Mechanical Engineering; juc16@psu.edu.

‡Distinguished Professor, Department of Mechanical Engineering; vigor@psu.edu. Fellow AIAA.

reactants delivered into the tubes at certain conditions, and the number of cycles needed to attain steady periodic operation in a multitube configuration is typically larger. Although this approach saves computational effort, the resultant error caused by model uncertainties is difficult to estimate and can be quite large. Ebrahimi et al.[9] conducted two-dimensional simulations for a dual-tube PDE, but only with single-pulse operation. They found that the pressure induced by the detonation in the neighboring tube is nearly as large as that produced by the detonation itself and that the shock wave produced by the detonation is sufficient to initiate combustion in the adjacent tube filled with fresh reactants. In a more recent work,[10] the effects of the tube number and length on the interactions among tubes were investigated based on single-pulse operation. The head-end pressure spike caused by the detonation wave from the adjacent tube can be reduced by increasing the number of tubes; however, an increase in tube length exerts no significant effect. To date, only the initial study by Ma et al.[11] and the very recent work by Ripley et al.[12] have simulated multitube PDEs with multicycle operations.

The present paper attempts to 1) develop a comprehensive numerical analysis dealing with the thrust chamber dynamics in multitube PDEs with repetitive operations, 2) examine the flow interaction among the detonation tubes, and 3) investigate the effects of operation timing and system geometry on the engine propulsive performance. The work represents an extension of our earlier study on single-tube airbreathing PDEs.[2]

II. Theoretical Model and Numerical Treatment

The basis of the present analysis is the model detailed in Ref. 2. Only a brief summary is given here. The analysis treats the full conservation equations of mass, momentum, energy, and species concentrations in two-dimensional coordinates and employs a chemical reaction scheme with a single progress variable calibrated for a stoichiometric hydrogen/air mixture. Diffusive effects are neglected. The governing equations and their associated boundary conditions are solved numerically using a recently developed space–time conservation element/solution element method.[13,14] Parallel computing is implemented based on the message-passing-interface library and a domain-decomposition technique for unstructured grids. All of the calculations were executed on an in-house personal-computer cluster consisting of 64 Pentium processors.

III. System Configuration

The PDE under consideration is shown schematically in Fig. 1. It includes a supersonic inlet with mixed compression, an air manifold, a rotary valve, a combustor consisting of multiple detonation tubes, and a common convergent-divergent (CD) nozzle. This engine was designed for a flight altitude of 9.3 km and a flight Mach number of 2.1. The static pressure and temperature of the freestream are 0.29 atm and 228 K, respectively, and the corresponding stagnation properties are 2.65 atm and 428 K. The total pressure at the entrance of the combustor is set to 2.12 atm based on a study of the inlet aerodynamics.[2,15] The flow interactions within the common manifold are represented by an additional 5% pressure loss for simplicity.[2]

The cyclic operation of the PDE is controlled by a rotary valve located at the entrance of the combustor. The detonation tubes operate sequentially with a fixed time lag, as shown schematically in Fig. 2 for a three-tube design. The head end of each tube is assumed to be either fully open or fully closed for simplicity. The operation of each individual tube is identical to that for a single-tube PDE[2] and is controlled by three time periods: the valve-closed period τ_{close} during which the valve is closed, the purging period τ_{purge} during

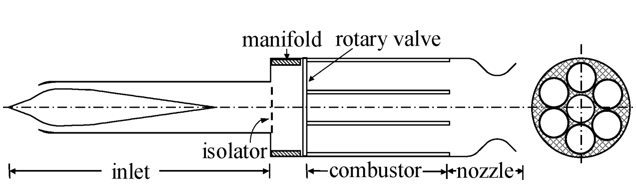

Fig. 1 Supersonic airbreathing pulse detonation engine.

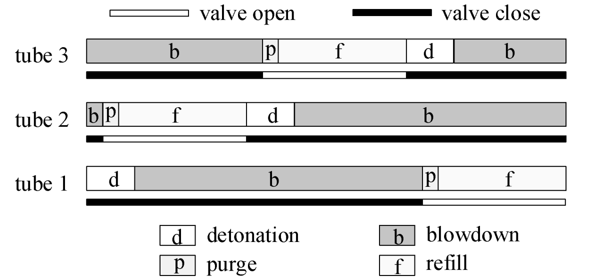

Fig. 2 Operation sequence of a triple-tube PDE.

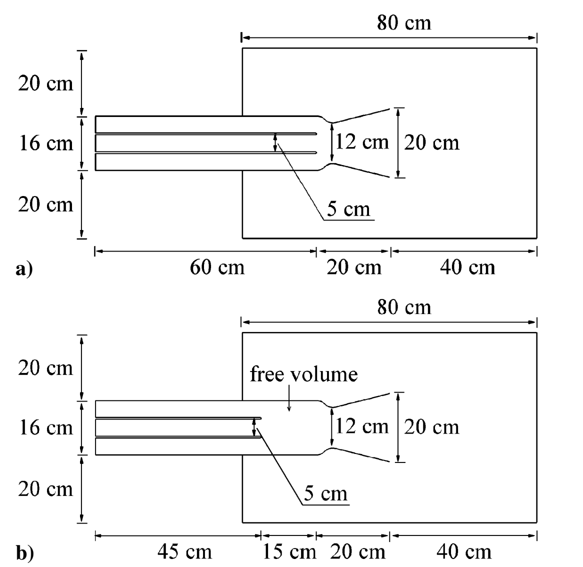

Fig. 3 Computational domains for multitube PDEs: a) without free volume and b) with free volume.

which a small amount of cold air is injected into the tube to prevent preignition of fresh reactants, and the refilling period τ_{refill} during which the combustible mixture is delivered to the tube. The cycle period for each tube τ_{cycle} is the sum of the preceding three periods, that is, $\tau_{cycle} = \tau_{close} + \tau_{purge} + \tau_{refill}$. Note that τ_{cycle} is usually greater than the engine cycle period by a factor equal to the number of detonation tubes.

Although the chamber dynamics in a practical multitube PDE are three dimensional, the present work considers only planar two-dimensional configurations. The emphasis of the study is on the interactions between the detonation tubes and the entire thrust chamber dynamics. The resultant flow phenomena and performance trends are believed to be qualitatively similar to those for three-dimensional cases. In addition, the two-dimensional analysis allows for a direct comparison with our earlier work on single-tube PDEs.[2] Figure 3 shows the computational domains for the two configurations considered herein. The combustor contains three detonation tubes spaced 0.5 cm apart. The height of the detonation tube is 5 cm, which is larger than the detonation cell size of around 2.5 cm for stoichiometric H_2/air at ambient pressure of 0.29 atm (Refs. 16 and 17), and thus permits successive propagation of detonation waves in the tube. The nozzle adopts the baseline shape used in Ref. 2, which measures a length of 20 cm and a throat height of 12 cm, along with a 45-deg half-convergent angle and a 15-deg half-divergent angle. In the first configuration, the detonation tubes have a length of 60 cm and extend to the nozzle entrance. In the second configuration, the length of the detonation tubes decreases to 45 cm, leaving a free volume of 15 cm long between the tubes and the nozzle. The same external region is included in the computational domains for both configurations. The numbers of unstructured grid cells for these two cases are 623,254 and 664,362, respectively. The grids were carefully selected to resolve detailed detonation propagation in the axial direction. They were further validated by conducting a grid-independence study of the computed solutions in terms of flow properties and propulsive performance.

The boundary conditions at the head end of the detonation tube are specified according to the stage in the engine operation cycle. It is modeled as a rigid wall when the valve is closed. During the purging stage, the total temperature and total pressure are specified as 428 K and 2.12 atm, respectively. The axial velocity is extrapolated from the interior points, and the reactant mass fraction is set to zero. The same conditions are used during the refilling stage, except that the reactant mass fraction is set to unity. A nonreflecting boundary condition is implemented along the open boundary of the external region.

IV. Results and Discussion

A series of simulations were conducted for both configurations over a wide range of operation parameters. Detailed flow evolution and engine propulsive performance were obtained, along with the identification of various loss mechanisms limiting the PDE performance.

A. Flow Evolution

The baseline case for the first configuration has an operation cycle period τ_{cycle} of 3 ms, giving rise to a time lag of 1 ms between tubes. The valve-closed time τ_{close}, purging time τ_{purge}, and refilling time τ_{refill} are 2.1, 0.1, and 0.8 ms, respectively, identical to those for the baseline single-tube case. The ambient flow is treated as stationary because of its negligible effect on the engine interior ballistics and propulsive performance.[2] Figure 4 shows the temporal evolution of the density-gradient field during the first cycle of operation. The corresponding pressure distribution along the centerline of each tube is given in Fig. 5, and the time histories of pressure at the center of the head end of each tube in Fig. 6.

Initially, the bottom tube is partially (75%) filled with a quiescent stoichiometric hydrogen/air mixture at the ambient pressure (0.29 atm) and temperature (228 K), with the remaining region filled with air. Detonation is directly initiated in the bottom tube by a driver gas spanning the tube 0.2 mm from the head end with a temperature of 2000 K and a pressure of 30 atm. This small amount of driver gas has a negligible contribution to the engine impulse.[2] The detonation

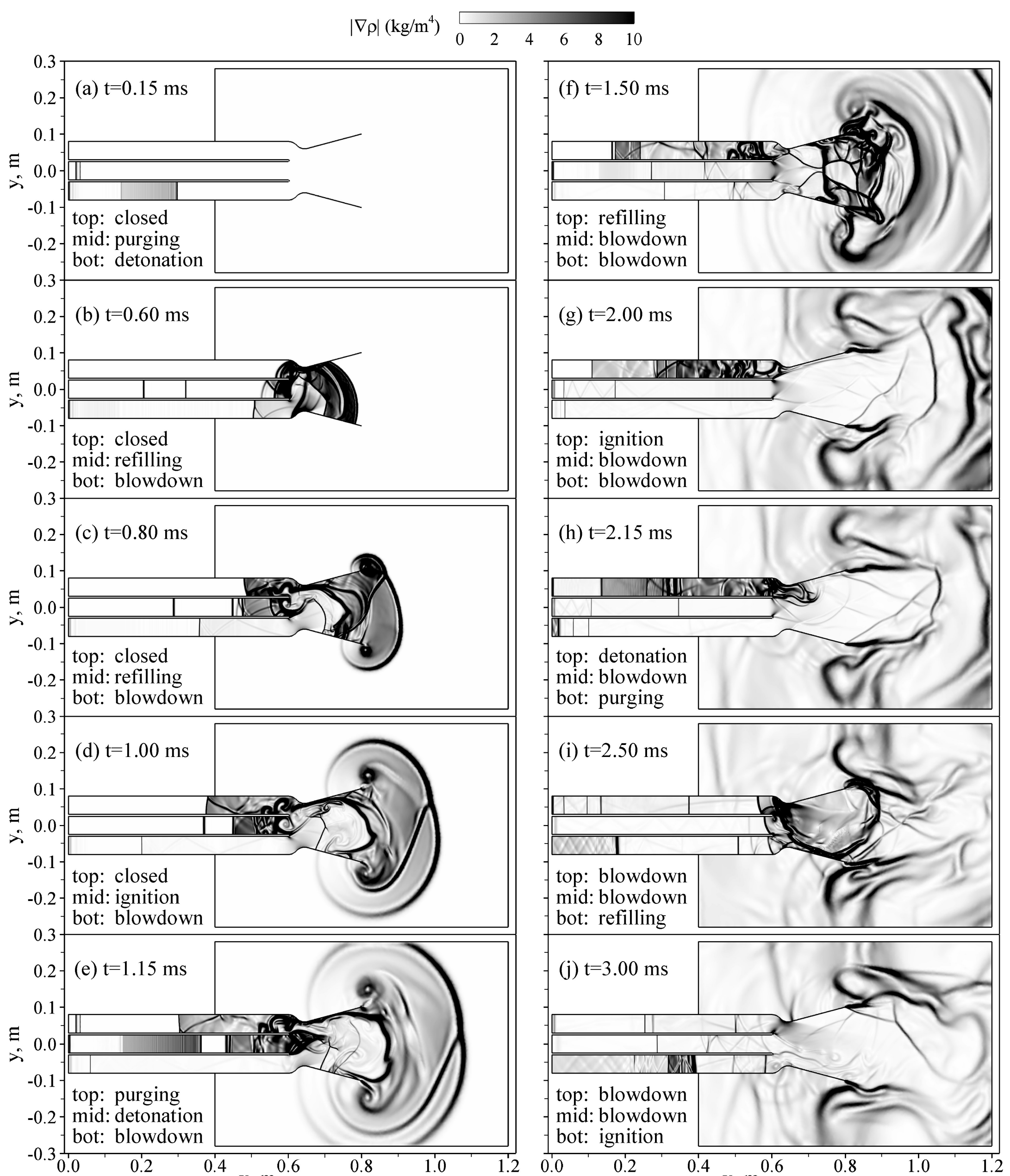

Fig. 4 Time evolution of density-gradient field during first cycle of operation ($\tau_{\mathrm{cycle}} = 3$ ms, $\tau_{\mathrm{close}} = 2.1$ ms, and $\tau_{\mathrm{purge}} = 0.1$ ms).

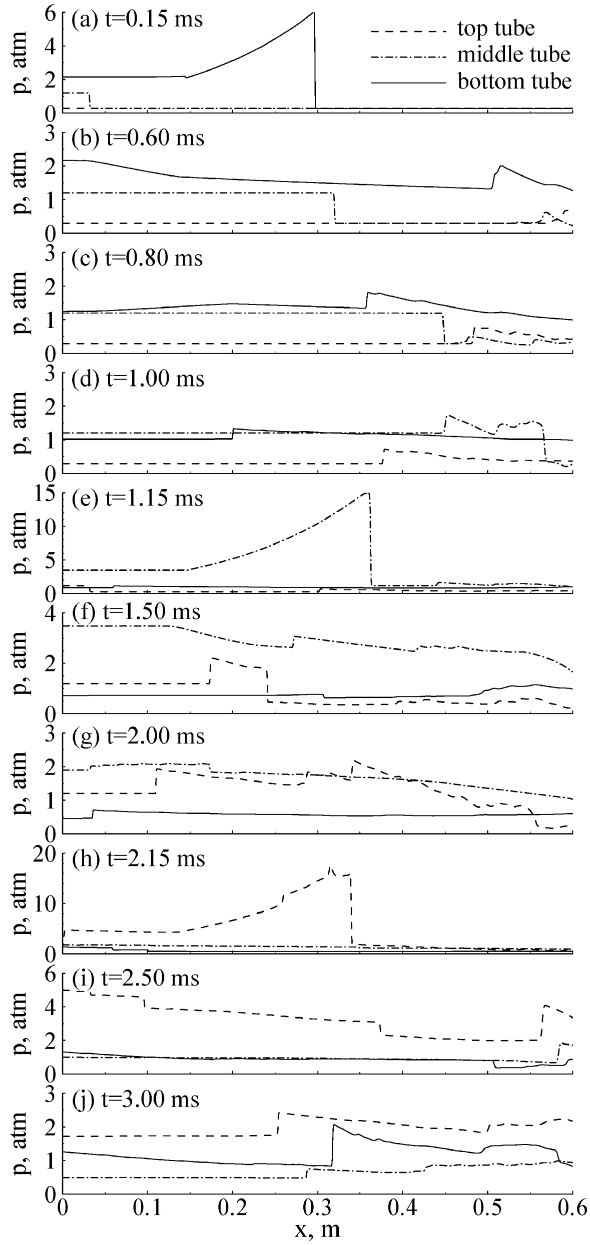

Fig. 5 Time evolution of pressure distribution along centerline of each tube during first cycle of operation for configuration without free volume ($\tau_{cycle} = 3$ ms, $\tau_{close} = 2.1$ ms, and $\tau_{purge} = 0.1$ ms).

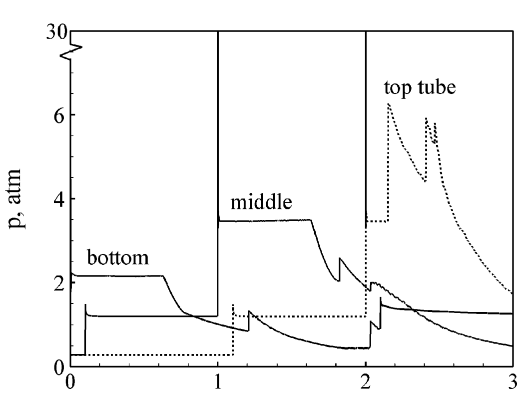

Fig. 6 Time histories of pressure at centers of head ends of detonation tubes during first cycle of operation for configuration without free volume ($\tau_{cycle} = 3$ ms, $\tau_{close} = 2.1$ ms, and $\tau_{purge} = 0.1$ ms).

wave then propagates downstream at the Chapman–Jouguet (CJ) speed of 1956 m/s, followed by the Taylor expansion wave and a uniform region, as discussed comprehensively in Refs. 1 and 2. The CJ pressure and temperature are 5.855 atm and 2663 K, respectively, whereas the pressure and temperature in the uniform region are 2.158 atm and 2133 K, respectively. At $t = 0.15$ ms, the detonation wave has traveled approximately one-half of the tube length, and the uniform region spreads about halfway between the detonation wave front and the head end. The middle tube is in the purging stage. The two vertical lines in Fig. 4a represent the shock wave and the contact surface induced by the pressure difference across the valve when the purging process begins. The pressure and velocity behind the shock wave are 1.20 atm and 411 m/s, respectively.

The detonation wave in the bottom tube reaches the reactant/air interface located 40 cm from the head end at $t = 0.20$ ms and then degenerates to a nonreacting shock wave (i.e., the primary shock wave). Meanwhile, a series of expansion waves are generated at the interface, propagating both downstream along with the Taylor wave to the tube exit and upstream to the head end. The upstream-traveling expansion waves interact and pass through the Taylor wave and thus reduce the length of the uniform region, as displayed in Fig. 5b. The first expansion wave arrives at the head end at $t = 0.625$ ms, and the head-end pressure begins to decay gradually (see Fig. 6). As the expansion waves reflect off the head end, another series of expansion waves form and propagate downstream toward the tube exit, further reducing the pressure in the bottom tube.

The primary shock wave reaches the bottom tube exit at $t = 0.380$ ms. It then diffracts at the tube exit and reflects from the nozzle walls, causing complex waves that propagate upstream into all the three tubes and downstream into the nozzle (see Fig. 4b). A close-up view of the flow development is given in Fig. 7. The primary shock wave is significantly weakened by the expansion waves before emerging from the bottom tube, with the pressure behind the shock decaying from 5.86 to 3.05 atm. The possibility of initiating detonation in the neighboring tubes is thus avoided. Figure 7b shows the flow structures related to the diffraction of the

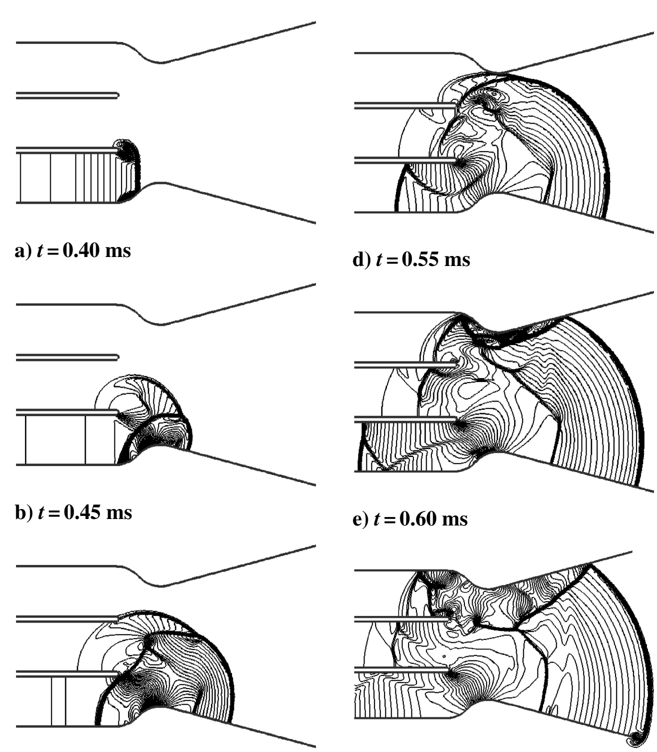

a) $t = 0.40$ ms

b) $t = 0.45$ ms

c) $t = 0.50$ ms

d) $t = 0.55$ ms

e) $t = 0.60$ ms

f) $t = 0.65$ ms

Fig. 7 Snapshots of pressure field showing flow interactions between tubes and nozzle during first cycle of operation ($\tau_{cycle} = 3$ ms, $\tau_{close} = 2.1$ ms, and $\tau_{purge} = 0.1$ ms).

shock wave around the upper edge of the bottom tube, including the Prandtl–Meyer expansion fan, the vortex formation, the secondary shock, and the shock reflected from the nozzle wall. At $t = 0.50$ ms, the diffracted and reflected shock waves have propagated into the middle and bottom tubes, respectively, and the pressures behind them are 0.32 and 2.40 atm. The diffracted shock is much weaker than the reflected one. The upper part of the leading shock hits the wall between the middle and top tubes, and its right branch propagates into the divergent section of the nozzle. Along the curved wall, the flow behind the leading shock is locally expanded to supersonic, leading to the formation of another shock wave stemming out from the wall, as evidenced in Fig. 7c. The upper part of the leading shock then reaches (Fig. 7d) and reflects off (Fig. 7e) the upper wall of the nozzle. The shock waves established in all three tubes propagate upstream and elevate the pressure therein (see Figs. 5b and 5c); however, their strength is not sufficient to initiate detonation. In both the middle and top tubes (Fig. 7e), the first shock diffracted from the bottom tube is much weaker than the second shock caused by the reflection from the lower wall of the nozzle. The convergent section of the nozzle helps preserve the chamber pressure, similar to the situation in the single-tube case.[2]

At $t = 0.80$ ms, the primary shock wave has emerged from the nozzle into the external region. Vortices are formed near the edges of the nozzle exit. The external flowfield exhibits a structure similar to that of the single-tube case,[2] except for its asymmetric structure. Within the chamber, the reflected shock in the bottom tube propagates toward the head end faster than those in the middle and top tubes because of the higher speed of sound associated with the high-temperature combustion products. The middle tube is still in the refilling stage. The shock wave generated in the purging process travels to $x = 45$ cm and is about to meet the upstream-traveling waves induced by the detonation in the bottom tube.

At $t = 1$ ms, the refilling process in the middle tube ends, and ignition occurs. The purge-induced contact surface arrives at $x = 37$ cm and the leading fresh reactant at $x = 32$ cm. The purge-induced shock interacts with the upstream-traveling waves induced by the detonation wave in the bottom tube. At $t = 1.15$ ms, the detonation wave in the middle tube reaches $x = 37$ cm. It propagates faster than that in the bottom tube because the reactants in the middle tube have already acquired a velocity of about 411 m/s prior to detonation. The top tube undergoes the purging process. At a slightly later time, the detonation wave in the middle tube catches the leading fresh reactant at $x = 39$ cm and degenerates to a nonreacting shock wave. The resultant wave then proceeds further downstream and interacts with the waves induced previously by the detonation wave in the bottom tube, causing a very complicated flow structure in the nozzle and the external region (see Fig. 4f). Two Prandtl–Meyer expansion fans are observed at the exit of the middle tube. The top tube is now in the refilling process, with a pressure of 1.20 atm and a velocity of 411 m/s. The interaction of the downstream- and upstream-traveling shock waves leads to a region with pressure up to 2.2 atm in the top tube (see Fig. 5f). To avoid interference from this high-pressure region, the refilling process should be finished before the upstream-traveling shock wave arrives at the head end. Otherwise, inlet overpressurization can happen. In the current case, the shock wave propagates at a speed of 126 m/s and reaches $x = 11$ cm when the refilling process ends.

Ignition occurs in the top tube at $t = 2$ ms, while the middle and bottom tubes undergo the blowdown process. The aforementioned shock wave travels through the detonation wave, and then reflects off the head end at about $t = 2.15$ ms, causing an abrupt rise in the head-end pressure, as evidenced in Fig. 6. At the same time, the detonation wave has passed through the leading fresh reactant at $x = 31.2$ cm and degenerated to a nonreacting shock wave. At $t = 2.5$ ms, the shock wave has exited from the nozzle and further interacts with the local flowfield in the external region. Reflected shock waves are observed near the exits of all of the three tubes. The pressures behind these shocks, from the bottom to the top tube, are 0.8, 1.8, and 4.0 atm, respectively. The bottom tube is in the refilling stage, with a pressure of 1.30 atm and a velocity of 380 m/s.

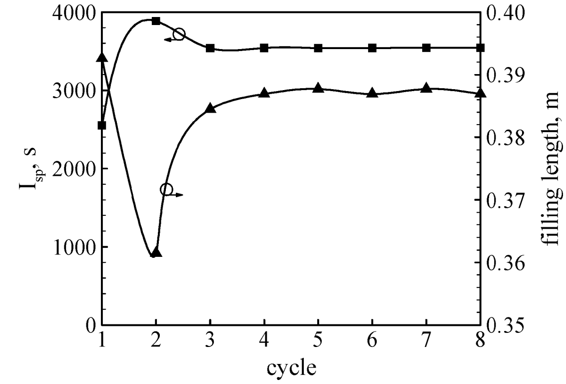

Fig. 8 Specific impulse and filling length of middle tube for first eight cycles ($\tau_{cycle} = 3$ ms, $\tau_{close} = 2.1$ ms, and $\tau_{purge} = 0.1$ ms).

The refilling process in the bottom tube finishes at $t = 3.0$ ms (the end of the first cycle). The leading fresh reactants reach $x = 35.5$ cm. In the middle and bottom tubes, the shock waves induced by the detonation wave in the top tube propagate further upstream and raise the local pressure, especially in the bottom tube (see Fig. 5j).

Compared with a single-tube PDE,[1,2] the present system features extremely complicated flow physics in the thrust chamber. The engine dynamics is dictated by the collective behavior of all of the detonation tubes and their interactions with the nozzle. The evolution of the flow downstream of the nozzle is also difficult to characterize using well-defined flow patterns (such as the Prandtl–Meyer expansion fan for an underexpanded nozzle flow and oblique shock waves for an overexpanded flow). The interwoven wave structures are further complicated by the transient operation of the engine, rendering efficient prediction of multitube PDE performance a challenging task.

The engine rapidly reaches its steady periodic operation as the cycle repeats. Figure 8 shows the temporal evolution of the specific impulse and the filling length of the middle tube. The former is calculated based on the momentum balance over a control volume enclosing the entire engine, as detailed in Ref. 2. The latter is defined as the length at which the detonation wave catches the leading fresh reactants. The specific impulse increases from the first to the second cycle as a result of the increasing loading density of the reactants and reaches a stable value of 3543 s at the eighth cycle. Figure 9 shows the time evolution of the density-gradient field during the eighth cycle. The corresponding pressure distribution along the centerline of each tube is given in Fig. 10. Quite different flow patterns from those in the first cycle are observed under the effect of flow nonuniformity arising from the preceding cycle. The flowfields at the beginning ($t = 21$ ms) and the end ($t = 24$ ms) of the cycle are identical, further confirming that the steady periodic operation has been reached. The averaged refilling pressures in the bottom, middle, and top tubes are 1.33, 1.11, and 1.28 atm, respectively, and the corresponding refilling velocities are 374, 435, and 386 m/s, respectively. The difference between the bottom and top tubes results from the operation sequence, although the bottom and the top tubes are located at mirror-reflected positions with respect to the engine centerline.

Figure 11 shows the time histories of the pressure at the centers of the head end and exit of each tube, to provide more quantitative information about the tube interactions. In Fig. 11a, the highest peak on each trace corresponds to the initiation of detonation at the head end. The second peak on the bottom-tube trace (point A) is attributed to the shock wave induced by the detonation in the top tube. The chamber is precompressed by shock waves originating from other tubes. Similarly, the second peak on the middle-tube trace (point B) corresponds to the shock wave induced by the detonation in the bottom tube. The same detonation wave also generates a shock wave that propagates into the top tube, interferes with the refilling process, and causes a small jump in the head-end pressure of the top tube, as denoted by point E. Because this pressure is still less than the total pressure of the incoming gas, the refilling process

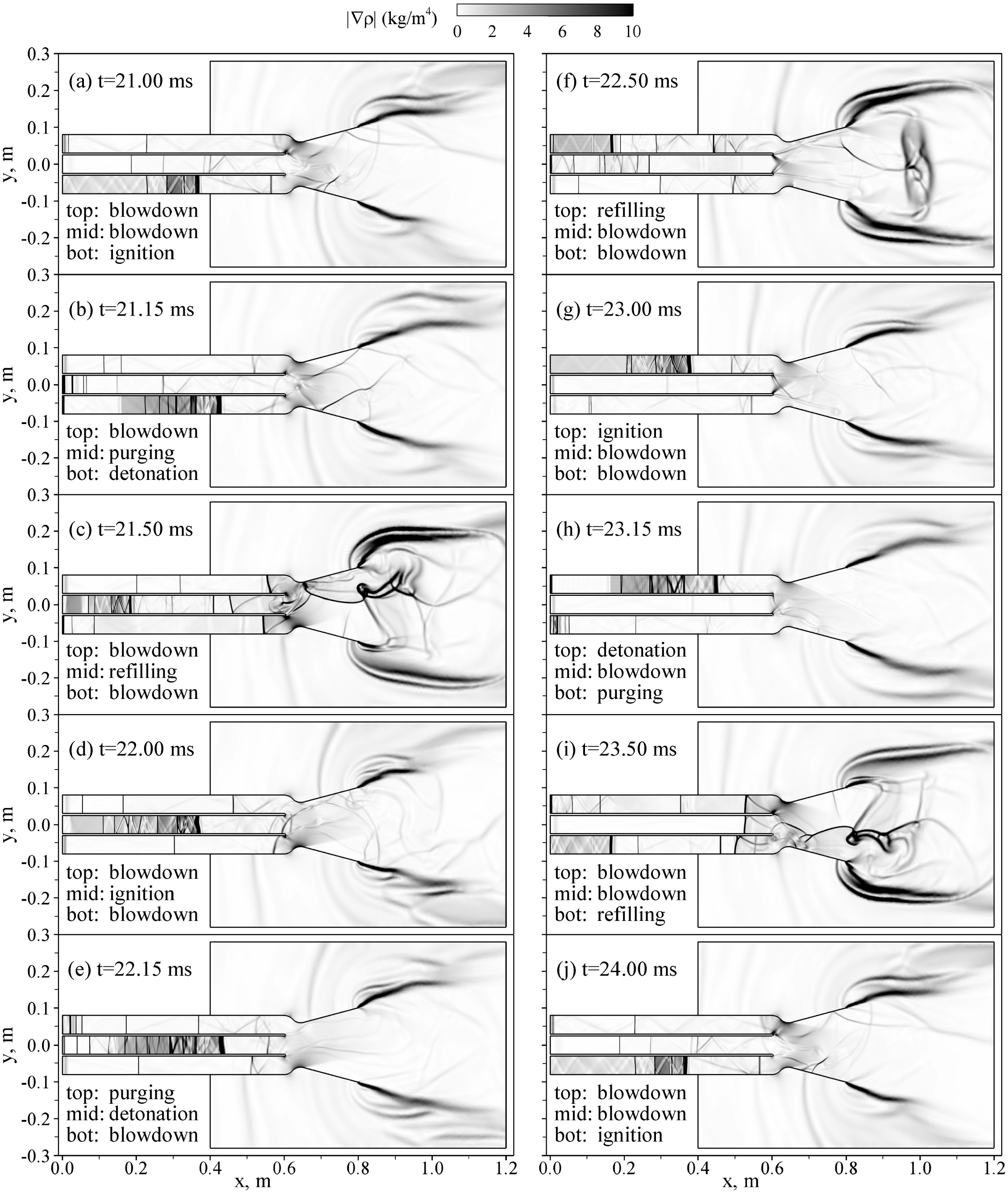

Fig. 9 Time evolution of density-gradient field during eighth cycle of operation ($\tau_{cycle} = 3$ ms, $\tau_{close} = 2.1$ ms, and $\tau_{purge} = 0.1$ ms).

continues. The second peak on the top-tube trace (point C) results from the detonation wave in the middle tube. The same detonation wave also causes a shock wave in the bottom tube that leads to a small jump in the head-end pressure (point F). The third peak (point D) corresponds to the arrival of the shock wave originating from the purge process in the middle tube, which, however, exerts little influence on the head-end pressure in the bottom tube. The latter phenomenon is attributed to the fact that the bottom tube is undergoing a supersonic flow exhaust when the purge-induced shock emerges from the middle tube. All of the pressure peaks (A, B, C, and D) exceed the total pressure of the incoming air and thus should be timed to occur within the valve-closed period. Otherwise, reversal flow can take place at the entrance of the detonation tubes and lead to engine unstart.

In Fig. 11b, the first peaks on the three pressure traces (points A, B, and C) correspond to the detonation-degenerated shock waves at the tube exits. The second peaks on the traces for the bottom and top tubes (points D and E) result from the arrival of the reflected shocks from the nozzle wall. The middle tube, however, does not experience this kind of pressure rise, because its exit is farther away from the nozzle wall, and a supersonic exhaust flow develops soon after the detonation-degenerated shock wave emerges from the middle tube.

The flow evolution within the nozzle, as shown in Fig. 9, is considerably different from that in a single-tube PDE.[2] The sequential operation of the detonation tubes gives rise to steep flow variations in the transverse direction involving complicated structures. The effect of the nozzle throat on the performance of the multitube PDE appears to be less important than on the single-tube configuration. The complexity of the nozzle flow is also evidenced in Fig. 12, in which the time histories of the Mach number at the centers of the nozzle throat and exit planes are displayed. For a single-tube

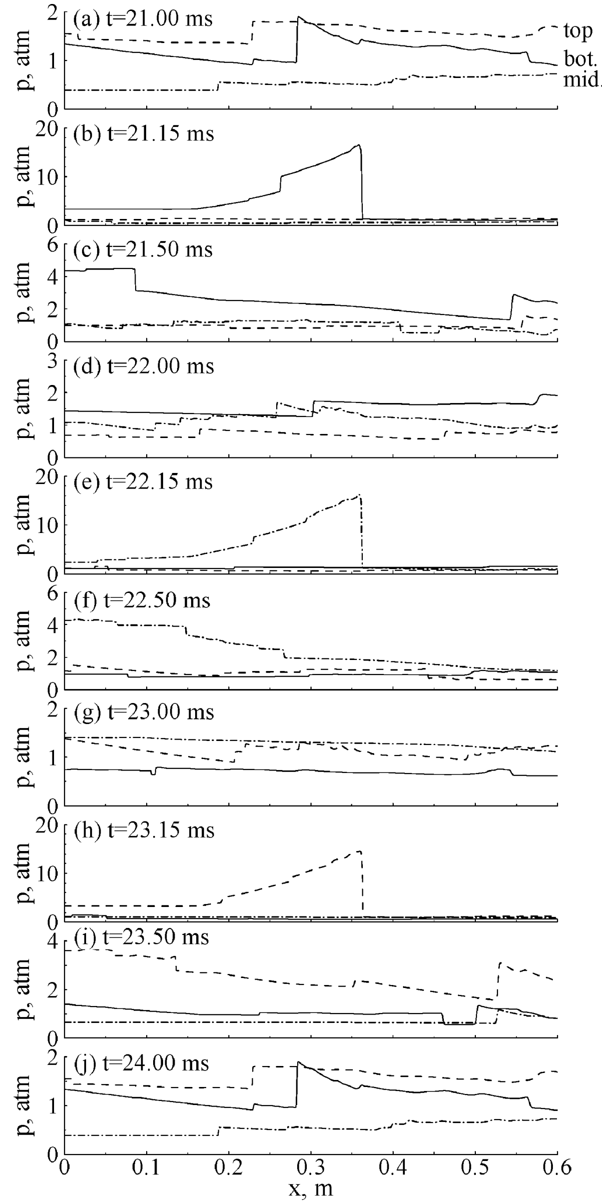

Fig. 10 Time evolution of pressure distribution along centerline of each tube during eighth cycle of operation (τ_{cycle} = 3 ms, τ_{close} = 2.1 ms, and τ_{purge} = 0.1 ms).

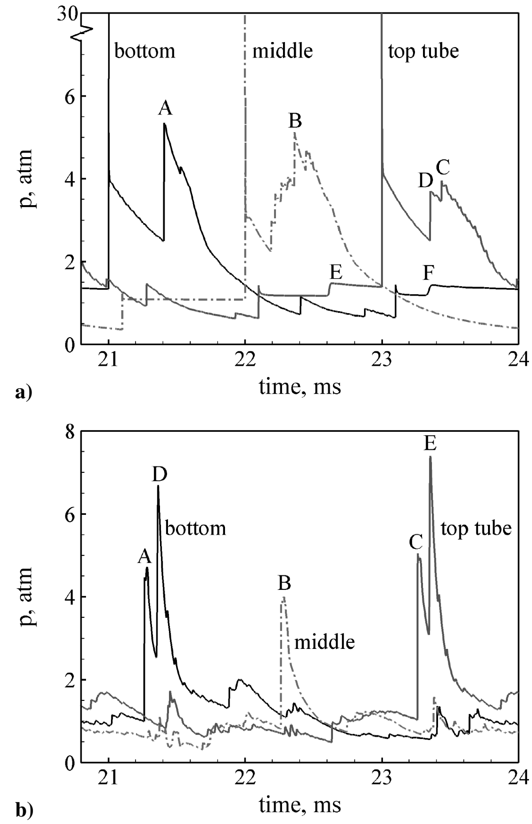

Fig. 11 Time histories of pressure at centers of a) head ends and b) exits of the bottom, middle, and top tubes during eighth cycle of operation (τ_{cycle} = 3 ms, τ_{close} = 2.1 ms, and τ_{purge} = 0.1 ms).

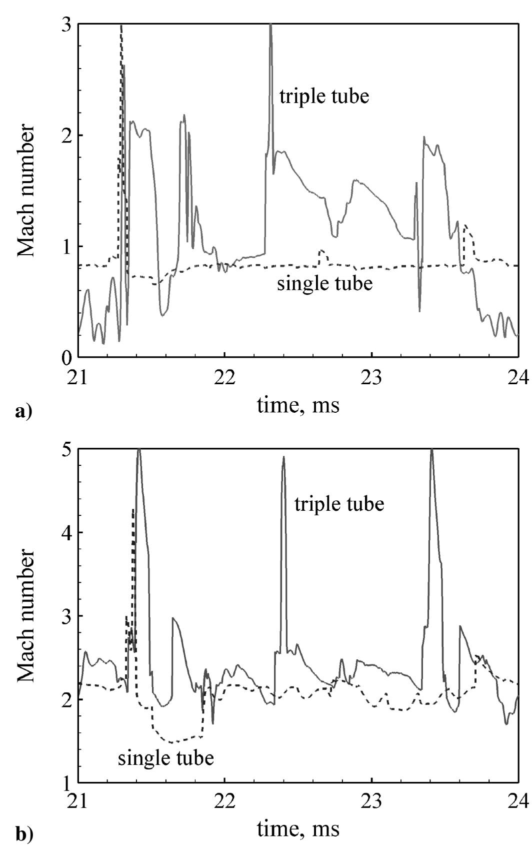

Fig. 12 Time histories of Mach number at centers of a) nozzle throat and b) nozzle exit during eighth cycle of operation (τ_{cycle} = 3 ms, τ_{close} = 2.1 ms, and τ_{purge} = 0.1 ms).

PDE, the nozzle is choked during the entire cycle except for a small period during which the detonation-degenerated shock wave travels through the throat region. The choke pattern typically includes a curved sonic line that starts at the wall slightly upstream of the throat and crosses the nozzle centerline downstream of throat. As a result, the Mach number at the center of the throat is slightly less than unity and remains almost unchanged during most of the cycle period. For a multitube PDE, however, the Mach number in the throat region undergoes rapid temporal and spatial variations and deviates substantially from unity. The choking effect of the nozzle throat is quite weak compared with the single-tube case for the same nozzle configuration and engine operating conditions. Figure 12b shows the evolution of the Mach numbers at the center of the nozzle-exit plane. The flow is supersonic throughout the entire cycle.

B. Propulsive Performance and Loss Mechanisms

The propulsive performance of a PDE must be determined appropriately. A detailed description of the performance calculation based on the momentum balance over the entire engine has been given in Ref. 2. Figure 13 shows the instantaneous thrust in both the axial and

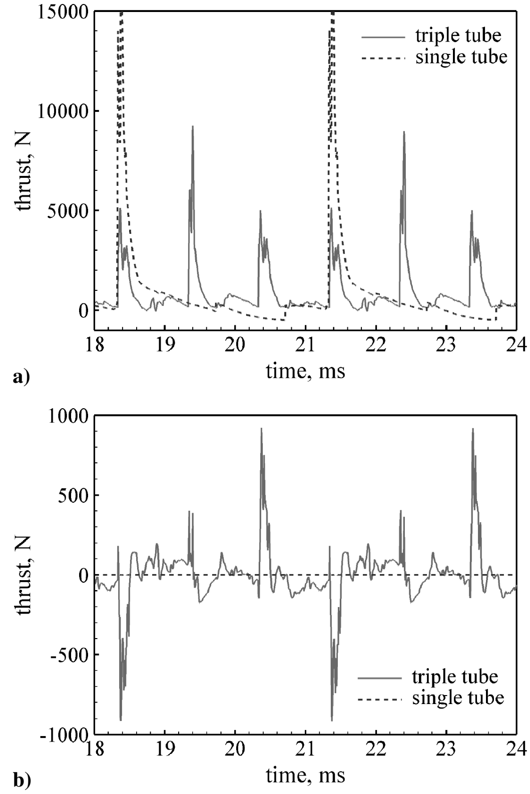

Fig. 13 Instantaneous thrust in a) axial and b) vertical directions during seventh and eighth cycles ($\tau_{\text{cycle}} = 3$ ms, $\tau_{\text{close}} = 2.1$ ms, and $\tau_{\text{purge}} = 0.1$ ms).

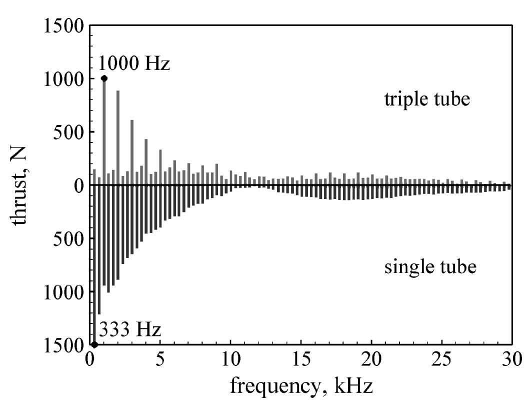

Fig. 14 Frequency spectra of axial thrust of single- and triple-tube PDEs with operation timing of $\tau_{\text{cycle}} = 3$ ms, $\tau_{\text{close}} = 2.1$ ms, and $\tau_{\text{purge}} = 0.1$ ms.

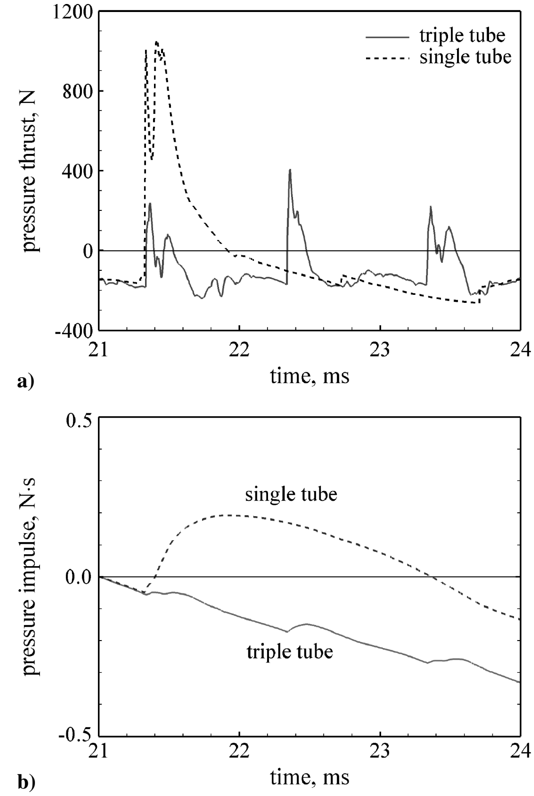

Fig. 15 Instantaneous pressure thrust and impulse during eighth cycle ($\tau_{\text{cycle}} = 3$ ms, $\tau_{\text{close}} = 2.1$ ms, and $\tau_{\text{purge}} = 0.1$ ms).

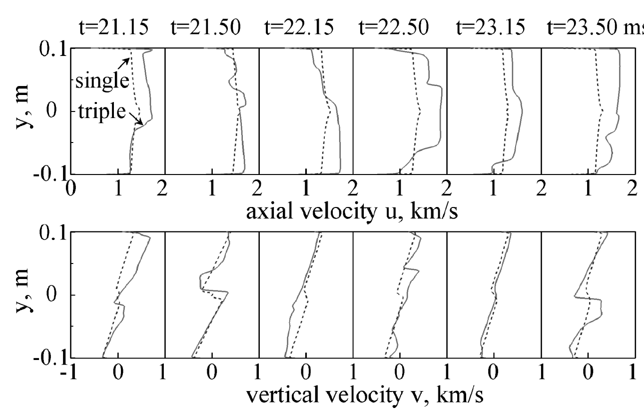

Fig. 16 Vertical distributions of axial and vertical velocities at nozzle-exit plane during eighth cycle of operation ($\tau_{\text{cycle}} = 3$ ms, $\tau_{\text{close}} = 2.1$ ms, and $\tau_{\text{purge}} = 0.1$ ms):—, triple tube; and —, single tube.

vertical directions, obtained from Eq. (17) of Ref. 2, with the time variation of the chamber momentum neglected. The counterpart results for the single-tube PDE are also included for comparison. As shown in Fig. 13a, there is a large spike up to 15,000 N for the single-tube case, corresponding to the arrival of the primary shock wave at the nozzle exit plane. For the present triple-tube design, the number of thrust peaks increases to three in each cycle, but the magnitude of the peaks is reduced almost by a factor of three. The deviation from the cycle-averaged value provides a quantitative measure of the engine thrust variation, so that the triple-tube design shows a substantial improvement in engine steadiness. The peaks occur when the detonation-degenerated shock waves in the bottom, middle, and top tubes arrive at the nozzle-exit plane. The second peak is higher than the others because the the middle tube is located at the axis, and the shock wave emerging from it experiences less diffraction and reflection and propagates more smoothly to the nozzle exit than those from the other two tubes. The peak in lateral thrust (see Fig. 13b) is smaller for the middle tube for the same reason. The increase in tube number modifies the spectral property of the thrust. Figure 14 shows the results for both the single- and triple-tube PDEs. The dominant frequency is equal to the product of the tube operating frequency and the number of tubes.

Figure 13a also shows that the time duration of negative thrust, caused by the low pressure and density at the nozzle exit, is significantly decreased to nearly zero for the triple-tube PDE. The deficiency associated with the low-energy exhaust flow during the later part of the blowdown stage and the refilling stage as encountered in a single-tube PDE is considerably alleviated in a multitube design through the sequential operation of the tubes. Figure 13b indicates the existence of lateral thrust up to 1000 N for the triple-tube PDE, which can cause unnecessary vibration of the vehicle. One way to mitigate this problem is to design the device using pairs of tubes located at mirror-reflected positions and operating synchronously in time to ensure symmetric operation. However, there can be situations in which lateral thrust could be desired to provide thrust vectoring.

The cycle-averaged specific impulse and thrust during steady periodic operation are 3543 s and 896 m/s, respectively. These performance numbers are about 4% higher than those of the baseline single-tube PDE given in Ref. 2. The multitube design slightly improves the propulsive performance.

To identify the various loss mechanisms, the flow-path-based analytical model proposed by Ma et al.[2] is used to predict the theoretical limit of PDE performance. The model requires specification of a refilling Mach number, which for the baseline case is 0.85, 1.0, and 0.94 for the bottom, middle, and top tubes, respectively. The average number of 0.93 coincides with that of the baseline single-tube PDE. The corresponding theoretical limit of the specific impulse is 4235 s, about 20% higher than the prediction from the present numerical simulation. According to the analysis outlined in Ref. 2, the thrust-chamber performance losses are attributed to the mismatch of the nozzle exit flow and the ambient condition, or nozzle expansion loss (∼3%), the nozzle flow divergence loss (∼2%), and the internal flow loss (∼15%). Compared with the single-tube case (a specific impulse of 3402 s with three losses of 6.1, and 16.5%), the triple-tube PDE improves the performance by 4%, mainly because of the substantial reduction in the nozzle expansion loss and a slight decrease in the internal flow loss. The nozzle flow divergence loss remains about the same for both configurations.

Figure 15 shows the instantaneous pressure thrust and impulse during a steady periodic cycle. The single-tube results are also included for comparison. In general, as for conventional steady engines, the magnitude of the pressure thrust should be minimized to optimize the efficiency of nozzle flow expansion. The triple-tube design offers better pressure matching at the nozzle exit than does the single tube. The pressure thrust shown in Fig. 15a indicates that the nozzle flow is predominantly overexpanded, unlike the single-tube case in which the underexpansion of the nozzle flow prevails, especially in the early stage of each cycle.

Nozzle flow divergence loss results from the angularity of the exhaust velocity vector. Figure 16 compares the velocity profiles of the triple- and single-tube PDEs at the nozzle-exit plane during a steady periodic cycle. The asymmetric pattern of the triple-tube results is clearly observed. The time-averaged magnitudes of both axial and vertical velocities are moderately higher than those of the single-tube PDE, and the flow divergence loss remains almost identical.

Internal flow loss is mainly attributed to the shock waves and their interactions within the thrust chamber. In spite of the intricate shock dynamics in a multitube PDE, the shock waves associated with the diffraction around the tube exit and the reflection from the nozzle wall are weaker than those in the single-tube case and produce a slightly smaller internal flow loss.

C. Effect of Operation Timing

The effects of operation timing on the engine propulsive performance were studied over a broad range of cycle τ_{cycle} and valve-closed τ_{close} times. The purge time τ_{purge} is fixed at 0.1 ms. Figure 17 shows the influence of τ_{close} on the air-based specific thrust F_{sp} and the fuel-based specific impulse I_{sp} for two cycle times of 3 and 4 ms. Steady cyclic operation is achieved after 8–12 cycles in most cases; in some cases, however, the cycle-averaged specific impulse continues to oscillate rather than reaching a stable value, as demonstrated in Fig. 18 for $\tau_{cycle} = 4.0$ ms. The case with $\tau_{close} = 2.4$ ms is a stable one, and the cases with $\tau_{close} = 1.8$ and 2.1 ms have relative oscillation magnitudes of about 2 and 1%, respectively. This phenomenon can be attributed to the intrinsic coupling between the unsteady flow dynamics and operation sequence.

The specific thrust increases as τ_{close} decreases for both frequencies considered herein, following the trend seen in single-tube PDEs, as discussed in Ref. 2. Briefly, for a given τ_{cycle} and τ_{purge}, a smaller τ_{close} leads to a higher loading density of fresh reactants and a larger quantity of reactants delivered to the chamber. The resultant shorter period of negative thrust and smaller internal flow loss gives rise to a higher specific thrust. The lower bound of τ_{close} is determined by three practical constraints.[2] The first is concerned with inlet overpressurization. The head-end pressure must not exceed the total pressure of the inlet air to allow for purging and refilling when the

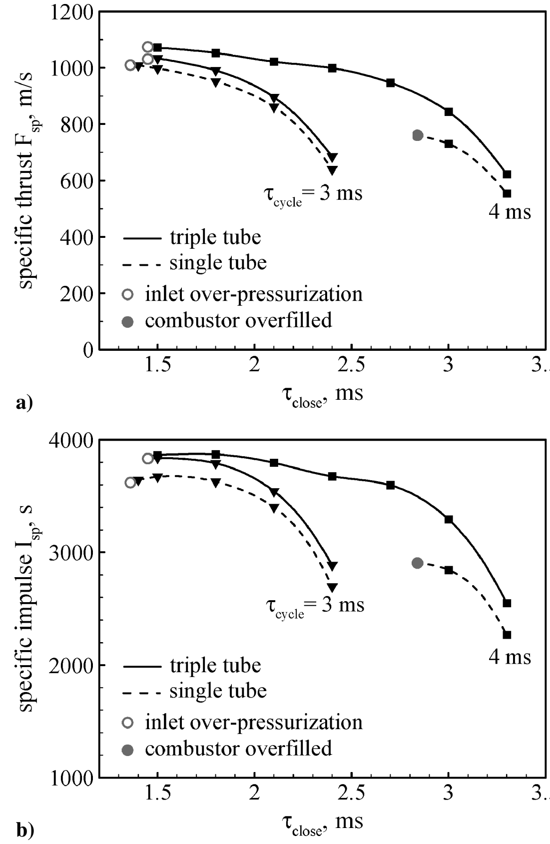

Fig. 17 Effect of valve-closed time on a) air-based specific thrust and b) fuel-based specific impulse: $\tau_{purge} = 0.1$ ms, stoichiometric H_2/air mixture, $h = 9.3$ km, $M_\infty = 2.1$.

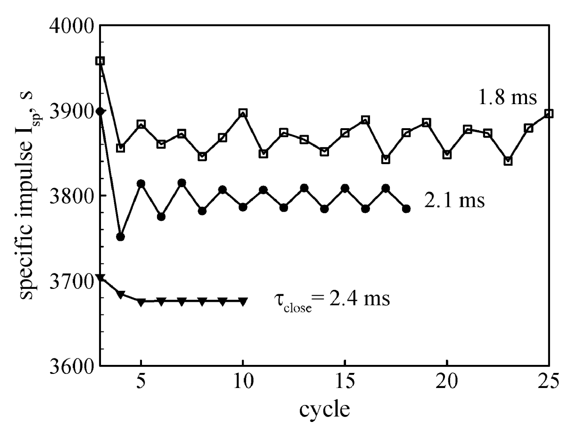

Fig. 18 Cycle-averaged specific impulse ($\tau_{cycle} = 4$ ms and $\tau_{purge} = 0.1$ ms).

valve is open. The second is related to chamber overfilling. The fresh reactants should not flow out of the nozzle to the external region before being burned completely unless afterburning is considered. The third is that τ_{close} should be sufficiently long to cover at least the time required for detonation initiation and propagation throughout the entire chamber. The upper bound of τ_{close} (also the lower bound of τ_{refill}) is determined by the requirement that an appropriate amount of fresh reactants be delivered to the chamber to produce thrust. The effect of τ_{close} on the specific impulse follows the same trend as that of the specific thrust, except for a small range of τ_{close} near its lower bound where the specific impulse can decrease as τ_{close} decreases.

In our previous study of single-tube PDEs,[2] it has been demonstrated that there exists an optimum frequency for a given engine configuration, which can be determined by the tradeoff between the following two conflicting effects: 1) more reactants can be recharged

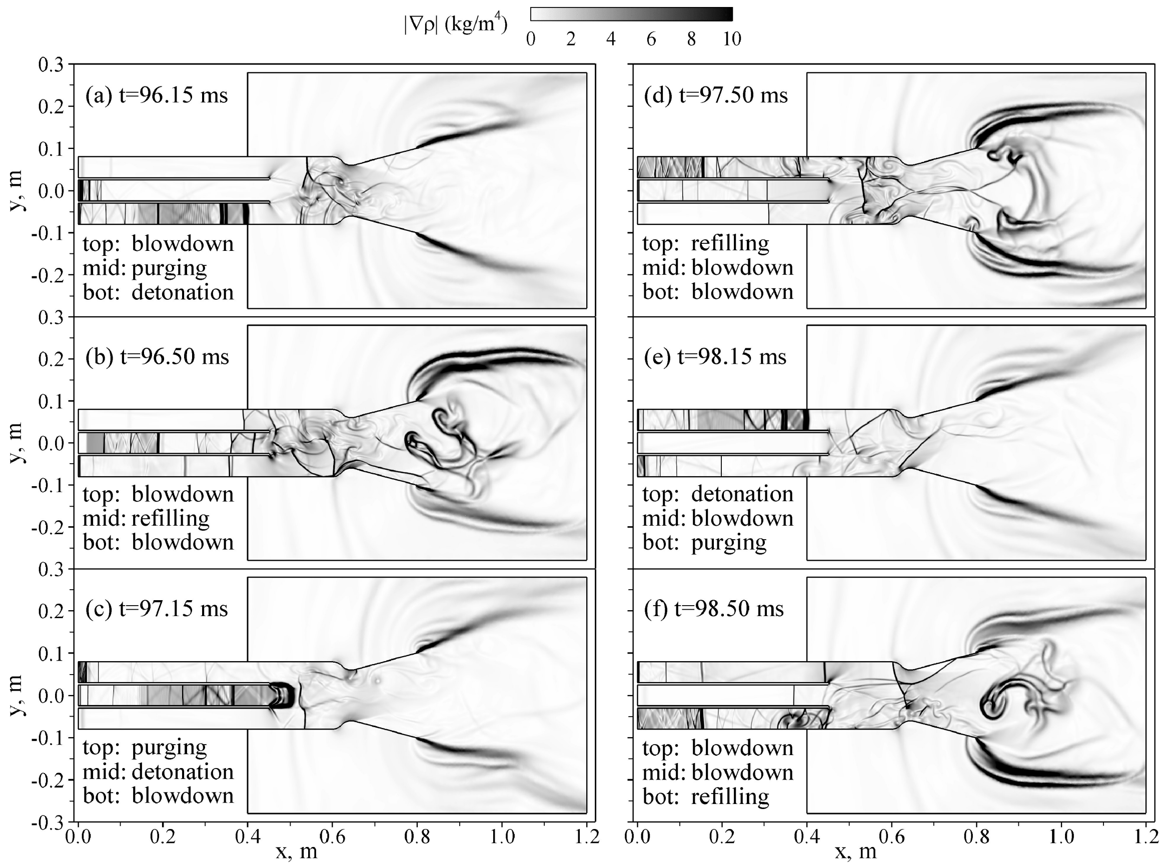

Fig. 19 Time evolution of density-gradient field during 33rd cycle of operation ($\tau_{\text{cycle}} = 3$ ms, $\tau_{\text{close}} = 2.1$ ms, and $\tau_{\text{purge}} = 0.1$ ms), with free volume.

into the detonation tube at a lower cycle frequency and 2) an exceedingly large refilling time associated with low-frequency operation can cause chamber overfilling and thus degrade the performance. A similar situation is found for multitube PDEs. Figure 17b indicates that the lower frequency of 250 Hz ($\tau_{\text{cycle}} = 4$ ms) offers not only a wider operating range but also a better performance. The best specific impulse obtained for the current design is 3870 s, with τ_{cycle} of 4 ms and τ_{close} of 1.8 ms. Further parametric studies are required to determine the optimum frequency for the present system.

Results of the propulsive performance shown in Fig. 17 demonstrate the superiority of the multitube design. For the 333-Hz operation, the specific impulse of the triple-tube PDE is about 4–5% higher than that of the single-tube PDE. For the 250-Hz operation, the triple-tube PDE offers both a wider operating range and a higher performance. The lower bound of τ_{close} encountered in the single-tube PDE as a result of combustor overfilling does not appear in the triple-tube case. Furthermore, performance improves as τ_{close} decreases until the lower bound associated with inlet overpressurization is reached. This phenomenon can be explained as follows. In a multitube PDE, the pressure in a detonation tube during the refilling process can be raised by the shock waves degenerated from the detonations in the other tubes, as discussed in Sec. IV.A. In contrast, the chamber pressure during the refilling process in a single-tube PDE can be quite low, especially for cases with extended blowdown periods. The resultant high refilling velocity and low loading density often lead to chamber overfilling and performance degradation.

D. Effect of System Geometry

In addition to operation timing, the engine configuration in terms of tube length and nozzle dimensions represents another important factor that affects both the flow dynamics and the propulsive performance of a multitube PDE. The effect of nozzle configuration has been investigated in our previous studies of single-tube PDEs.[2] The present work focuses on the effect of the free volume located between the detonation tubes and the common nozzle, as depicted in Fig. 3b. This region serves as a buffer zone to reduce the flow transients and mitigate the operation unsteadiness inherent in multitube operations.

Figure 19 shows the time evolution of the density-gradient field for a case with τ_{close} of 2.1 ms, τ_{refill} of 0.8 ms, and τ_{purge} of 0.1 ms. Steady periodic cycling is attained at the 33rd cycle , much later than the eighth-cycle benchmark for the baseline case without free volume. The average refilling pressures in the bottom, middle, and top tubes are 1.39, 1.01, and 1.02 atm, respectively, and the corresponding refilling velocities are 355, 466, and 461 m/s. The flow dynamics within the detonation tubes and in the external region bear a close resemblance to the case without free volume. The flowfield in the free volume, however, exhibits very complicated structures. In addition to the diffraction and reflection of the shock waves, the interactions between the supersonic exhaust flows from the detonation tubes with the subsonic flows in the corner regions near the nozzle entrance lead to the formation of high-intensity standing-like shock waves. For example, the shock wave located at the middle of the free volume (see Fig. 19d) has a pressure ratio of as high as five. It does not propagate back into the detonation tubes and raise the pressure there, but rather contributes to the internal flow loss. The unsteady flow recirculation, as evidenced in Fig. 20, represents another loss mechanism and degrades the performance.

Figure 21 shows the instantaneous axial thrust during a steady periodic cycle for configurations with and without free volume. The second peak, related to the detonation in the middle tube, is slightly reduced by adding the free volume, whereas the first and third peaks, related to the detonations in the other two tubes, remain about the same. The improvement in operation steadiness for the case with free volume appears to be quite limited. The specific impulse and specific thrust are 3372 s and 855 m/s, respectively, about 5% lower than those without free volume. Following the analysis developed in Ref. 2, the performance losses are identified to include

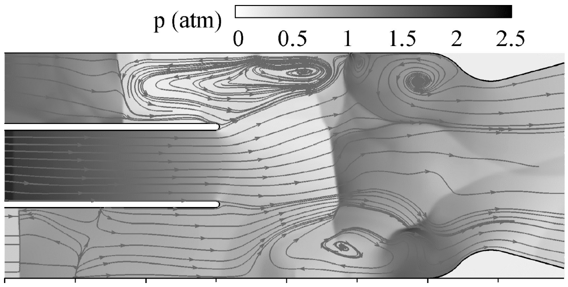

Fig. 20 Pressure contours and streamlines in system with free volume at t = 97.50 ms ($\tau_{\mathrm{cycle}} = 3$ ms, $\tau_{\mathrm{close}} = 2.1$ ms, and $\tau_{\mathrm{purge}} = 0.1$ ms).

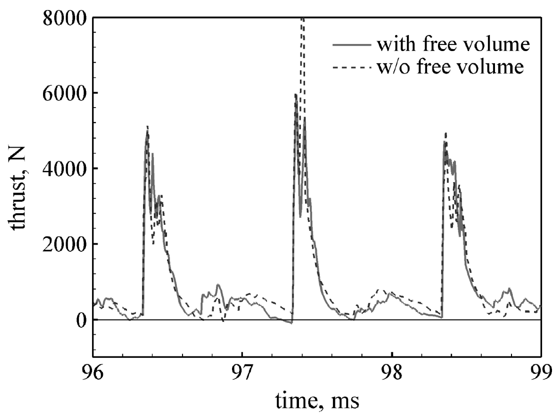

Fig. 21 Instantaneous axial thrust during steady periodic cycle ($\tau_{\mathrm{cycle}} = 3$ ms, $\tau_{\mathrm{close}} = 2.1$ ms, and $\tau_{\mathrm{purge}} = 0.1$ ms).

nozzle expansion loss of 2%, nozzle flow divergence loss of 2% and internal flow loss of 21%. Compared with the baseline case, the free volume slightly reduces the nozzle expansion loss, but significantly increases the internal flow loss caused by the complicated shock waves and the recirculation zones within the free volume. The nozzle flow divergence loss remains about the same for both cases.

V. Summary

The thrust chamber dynamics in multitube airbreathing pulse detonation engines (PDEs) with repetitive operations has been studied numerically over a broad range of operating parameters. Detailed flow evolution was examined, and loss mechanisms were quantified. Emphasis was placed on the interactions between detonation tubes and their collective influence on the nozzle flowfield. The benefits of precompression of refilled fresh reactants by shock waves originating from other tubes were demonstrated. The general behavior and propulsive performance of multitube PDEs were found to be similar to those of single-tube designs. For a given cycle period and purge time, the performance increases with decreasing valve-closed time. In addition, there exists an optimum frequency for achieving maximum thrust and specific impulse. Multitube PDEs improve the propulsive performance and operation steadiness and offer a wider operation range in terms of valve timing. The free volume between the detonation tubes and the common nozzle helps reduce the nozzle expansion loss and suppress flow oscillations. The associated complicated shock structures and recirculating flows, however, elevate the internal flow loss.

Acknowledgments

This work was supported by the U.S. Department of Defense Multidisciplinary University Research Initiative under the Office of Naval Research Grant N00014-02-1-0589, with Gabriel Roy serving as the program manager. The second author, J. Y. Choi, was partly supported by the Postdoctoral Fellowship Program of the Korea Science and Engineering Foundation.

References

[1] Wu, Y. H., Ma, F. H., and Yang, V., "System Performance and Thermodynamic Cycle Analysis of Airbreathing Pulse Detonation Engines," *Journal of Propulsion and Power*, Vol. 19, No. 4, 2003, pp. 556–567.

[2] Ma, F. H., Choi, J. Y., and Yang, V., "Thrust Chamber Dynamics and Propulsive Performance of Single-Tube Pulse Detonation Engines," *Journal of Propulsion and Power*, Vol. 21, No. 3, 2005, pp. 512–526.

[3] Goddard, R. H., "Rotating Valve for Multiple Resonance Combustion Chambers," Patent No. 2515644, 18 July 1950.

[4] Bussing, T. R. A., "A Rotary Valve Multiple Pulse Detonation Engine (RVMPDE)," AIAA Paper 1995-2577, July 1995.

[5] Bratkovich, T. E., and Bussing, T. R. A., "A Pulse Detonation Engine Performance Model," AIAA Paper 1995-3155, July 1995.

[6] Hinkey, J. B., Williams, J. T., Henderson, S. E., and Bussing, T. R. A., "Rotary-Valved, Multiple-Cycle, Pulse Detonation Engine Experimental Demonstration," AIAA Paper 1997-2746, July 1997.

[7] Schauer, F., Stutrud, J., and Bradley, R., "Detonation Initiation Studies and Performance Results for Pulsed Detonation Engine Applications," AIAA Paper 2001-1129, Jan. 2001.

[8] Mohanraj, R., Merkle, C. L., and Ebrahimi, H. B., "Modeling of Pulse Detonation Engine Operation," AIAA Paper 2001-0475, Jan. 2001.

[9] Ebrahimi, H. B., Mohanraj, R., and Merkle, C. L., "Modeling of Multi-Tube Pulse Detonation Engine Operation," AIAA Paper 2001-3813, July 2001.

[10] Ebrahimi, H. B., Malo-Molina, F. J., and Merkle, C. L., "Numerical Investigation of Multi-Tube Pulse Detonation," AIAA Paper 2003-0718, Jan. 2003.

[11] Ma, F. H., Choi, J. Y., Wu, Y. H., and Yang, V., "Modeling of Multitube Pulse Detonation Engine Dynamics," *Confined Detonations and Pulse Detonation Engines,* edited by G. Roy, S. Frolov, R. Santoro, and S. Tsyganov, Torus Press, Moscow, 2003, pp. 233–248.

[12] Ripley, R. C., Harris, P. G., and Farinaccio, R., "Multi-Tube Two-Dimensional Evaluation of a Pulse Detonation Engine as a Ramjet Replacement," AIAA Paper 2004-3745, July 2004.

[13] Wang, X. Y., and Chang, S. C., "A 2D Non-Splitting Unstructured Triangular Mesh Euler Solver Based on the Space-Time Conservation Element and Solution Element Method," *Computational Fluid Dynamics Journal*, Vol. 8, No. 2, 1999, pp. 309–325.

[14] Wu, Y. H., Ma, F. H., and Yang, V., "Space-Time Method for Detonation Problems with Finite-Rate Chemical Kinetics," *International Journal of Computational Fluid Dynamics*, Vol. 18, No. 3, 2004, pp. 277–287.

[15] Oh, J. Y., Ma, F. H., Hsieh, S. Y., and Yang, V., "Interactions Between Shock and Acoustic Waves in a Supersonic Inlet Diffuser," *Journal of Propulsion and Power*, Vol. 21, No. 3, 2005, pp. 486–495.

[16] Bull, D. C., Elsworth, J. E., Shuff, P. J., and Metcalfe, E., "Detonation Cell Structures in Fuel/Air Mixtures," *Combustion and Flame*, Vol. 45, 1982, pp. 7–22.

[17] Stamps, D. W., and Tieszen, S. R., "The Influence of Initial Pressure and Temperature on Hydrogen-Air-Diluent Detonations," *Combustion and Flame*, Vol. 83, No. 3, 1991, pp. 353–364.